J Therm Anal Calorim (2010) 99:45–50
DOI 10.1007/s10973-009-0543-0

# Dynamical properties of ethylene glycol and glucose studied by temperature-modulated differential scanning calorimetry and Brillouin scattering

**Eiji Hashimoto · Yuichi Seshimo · Keita Sasanuma · Yuichiro Aoki · Hitoshi Kanazawa · Yuji Ike · Seiji Kojima**

Japan Symposium 2008


**Abstract** The fragility of ethylene glycol and glucose aqueous solution systems has been investigated by temperature-modulated differential scanning calorimetry (TMDSC). The frequency and temperature dependences of complex specific heat have been observed in the vicinity of a glass-transition temperature $T_g$. It is shown that the value of the fragility index $m$ can be determined from the temperature dependence of the α-relaxation times observed by TMDSC. We have also studied the elastic properties of these aqueous solutions by micro-Brillouin scattering, and determined these relaxation times of elastic properties in the gigahertz range.

**Keywords** Brillouin scattering · Cryoprotectant · Fragility · TMDSC

## Introduction

Vitrification provides a general solution to the problem of organ preservation, because it allows avoiding both the direct and the indirect damaging effects of freezing. Generally, water in a cell crystallizes below a melting point, and ice crystals cause the destruction of cells. This is a serious problem [1, 2]. Cryoprotectant is a material that enables cells to cryopreserve. Particularly, glassy states of lower alcohols and saccharides are found in nature as cryoprotectants of biological tissues and life itself [3–5]. Ethylene glycol (EG) and glucose aqueous solutions are well-known cryoprotectants. In addition, recently, the research from the difference of the concentration dependence of the density between alcohol and glucose aqueous solutions has been reported [6]. Therefore, alcohol and glucose are now widely watched and it is very important to investigate the different nature of glass transitions of EG and glucose aqueous solutions is very important [7, 8].

Dynamics of supercooled liquid and glass transition has been one of the central issues in materials sciences. In a glass-forming liquid, a characteristic relaxation time of α-relaxation related to the cooperative rearrangement process in liquid drastically increases near a glass-transition temperature $T_g$. To understand the origin of the remarkable slowing down of the relaxation dynamics near $T_g$ is an important challenge [9].

In order to classify variations of the structural relaxation process (α-relaxation), the concept of "fragility" is introduced by Angell [10]. The classification is based on the scaled-Arrhenius plot for a temperature dependence of viscosity or relaxation time $\tau(T)$ or viscosity. "Strong" liquids obey the Arrhenius law, whereas "fragile" liquids display pronounced deviations from the Arrhenius law as temperatures approach $T_g$. To evaluate degrees of fragility in a more quantitative way, the fragility index $m$ is used defined by

$$m = \left| \frac{\mathrm{d} \log_{10} \tau}{\mathrm{d}\left(T_g/T\right)} \right|_{T=T_g} \quad (1)$$

In other words, a value of $m$ is determined as the slope of the $\tau(T)$ curve *at* $T = T_g$ in the Angell plot.

Micro-Brillouin spectroscopy has been the reliable method of a noncontact micro-probe for elastic properties [11, 12]. The Brillouin-scattering measurement enables us to determine the sound velocity, elastic constants, and

E. Hashimoto · Y. Seshimo · K. Sasanuma · Y. Aoki · H. Kanazawa · Y. Ike · S. Kojima (✉)
Graduate School of Pure and Applied Sciences, University of Tsukuba, Tsukuba, Ibaraki 305-8573, Japan
e-mail: kojima@bk.tsukuba.ac.jp

damping of sound waves. It is known to be a powerful tool to explore the elastic property in the high-frequency gigahertz range and in the extremely wide temperature range. Furthermore, Brillouin scattering is one of the measurement techniques of glass-transition process [13].

In this study, the dynamical properties of giga- and millihertz ranges of EG and glucose aqueous solutions as cryoprotectants were examined by temperature-modulated differential scanning calorimetry (TMDSC) and micro-Brillouin scattering. Especially, under the gigahertz range, we examined these dynamics in wide temperature range nothing so much up to now.

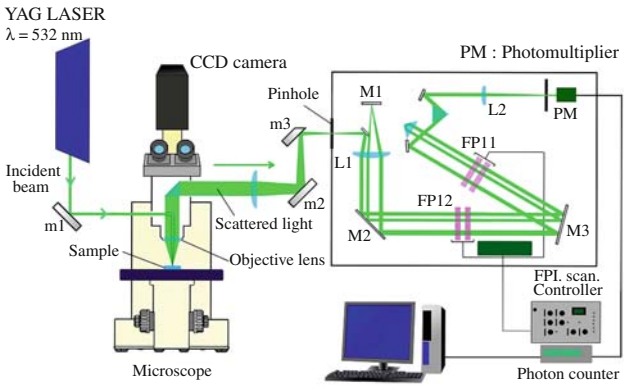


**Fig. 1** Schematic diagram of the micro-Brillouin scattering instrument

## Experimental

Thermal analysis was done by TMDSC technique, performed by TA instruments MDSC 2920, Q200 with Liquid Nitrogen Cooling Accessory. The temperature, the enthalpy, and the phase angle calibrated by the method described in Ref. [14]. We investigated thermal relaxation around a glass-transition temperature ($T_g$) on EG aqueous solutions (50 and 70 mol%) by DSC2920. The underlying heating rate was 0.5 °C/min, modulation amplitude ±0.2 °C, modulated period 100, 60, and 40 s. We investigated thermal relaxation under glucose aqueous solutions (15 and 25 mol%) around a glass-transition temperature ($T_g$) by Q200. The underlying heating rate was 0.5 °C/min, modulation amplitude ±1.0 °C, modulated period 180, 160, 140, 120, 100, 80, and 60 s.

The gigahertz elastic property was measured by Brillouin scattering [15]. The exciting source was a single frequency green YAG laser ($\lambda = 532$ nm, 50 mW). The Brillouin-scattering spectra were measured at the backward scattering geometry using the Sandercock-type 3 + 3 pass tandem Fabry-Perot Interferometer (FPI). Brillouin spectra were recorded in the frequency range of ±25 GHz with a free spectral range of 30 GHz. The sample temperature in a cryostat cell (LINKAM HTMS600) was controlled from −170 °C to 200 °C. The temperature stability was within ±0.1 °C in the whole experiments. We studied elastic properties of EG aqueous solutions (40, 50, and 70 mol%), pure glucose (glassy glucose), and glucose aqueous solutions (15, 20, and 25 mol%) using micro-Brillouin scattering as shown in Fig. 1.

## Results and discussion

### Thermal properties

TMDSC measurement is the extension of the heat flux type of conventional DSC; thus, the measured quantity is the temperature difference between sample and reference. The temperature difference converts into the differential heat flow. Resultant heat flow is analyzed by the deconvolution of the sample's response into underlying heating rate. The raw resultant heat flow (HF) is averaged over the period of more than one modulation. Then the averaged heat flow is subtracted from the resultant HF, the modulated component to the resultant HF is obtained. This modulated component is analyzed by the discrete Fourier transformation (DFT) to obtain the amplitude of heat flow modulation ($A_{MHF}$), and the phase lag ($\varphi$) between the modulation in the heat flow and the heating rate. The correction of the phase angle is performed by the method described in Ref. [14]. The $C_p^*(\omega)$ is defined as the ratio of $A_{MHF}$ and the amplitude of modulation in the heating rate ($A_{Mq}$).We can separate $C_p^*(\omega)$ into the real $C_p'$ and the imaginary $C_p''$ parts using phase lag ($\varphi$) by

$$C_p' = \left|C_p^*(\omega)\right| \cos\varphi, \tag{2}$$

$$C_p'' = \left|C_p^*(\omega)\right| \sin\varphi, \tag{3}$$

where $C_p'$ relates to an in-phase component of the modulation and $C_p''$ relates to an out-of-phase component. Figure 2 shows the $C_p'$ and $C_p''$ of the EG aqueous solutions as a function of temperature in the vicinity of $T_g$. The frequency of the applied temperature modulation to the system is fixed and the relaxation times of the studied sample drastically change as a function of temperature. As shown in Fig. 2, the curve of $C_p'$ indicates a step-like behavior and $C_p''$ has a peak around $T_g$. Both of them are the characteristic features of the complex susceptibility of a relaxation process.

The change of the frequency of the modulation enables us to investigate a frequency dependence of complex specific heat. Figure 3 shows the frequency dependences of EG 50-mol% aqueous solution of the $C_p'$ and $C_p''$. The peak temperature of $C_p''$ shifts higher as the modulation period

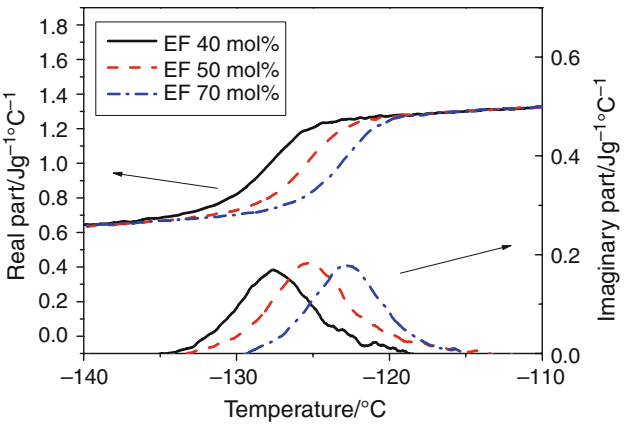


**Fig. 2** Real and imaginary parts of complex specific heat of EG aqueous solutions (modulation period is 100 s)

becomes shorter. The characteristic relaxation time $\tau$ of the system is the most probable at the peak temperature with the constant modulation period $P$. Relaxation time $\tau$ can be given by

$$\tau = \frac{1}{\omega} = \frac{P}{2\pi}. \tag{4}$$

By plotting the obtained $\tau$ of each frequency by $T$, values of $\tau(T)$ were obtained. The obtained values of $\tau(T)$ of EG 50- and 70-mol% aqueous solutions and glucose 15- and 25-mol% aqueous solutions are plotted against $T_g$-scaled reciprocal temperature, as shown in Figs. 4 and 5. The $T_g$ is defined as the temperature when $\tau$ becomes 100 s. All measurements were carried out with the most reliable experimental condition of $\tau = 100$ s according to our experience. The value of $T_g$ is calculated by the extrapolation from the present experimental data.

The fragility index $m$ defined by Eq. 1 is determined by a slope of $\tau(T)$ in Figs. 4 and 5 under the assumption of the linear evolution. This assumption is valid in this study,

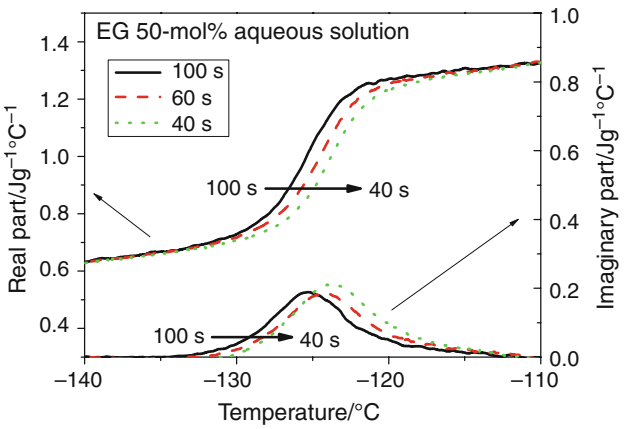


**Fig. 3** Frequency dependence of complex specific heat of EG 50 mol%

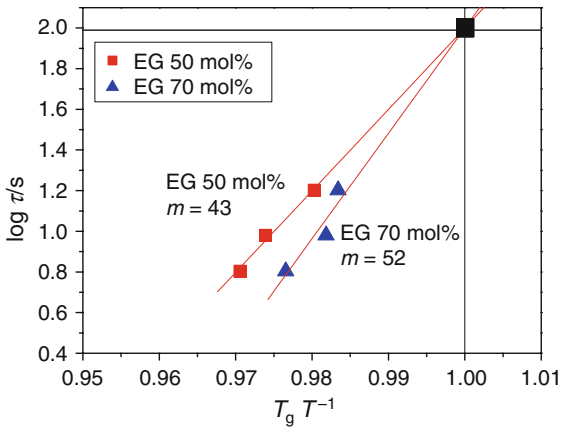


**Fig. 4** Angell plot of EG aqueous solutions (50 and 70 mol%)

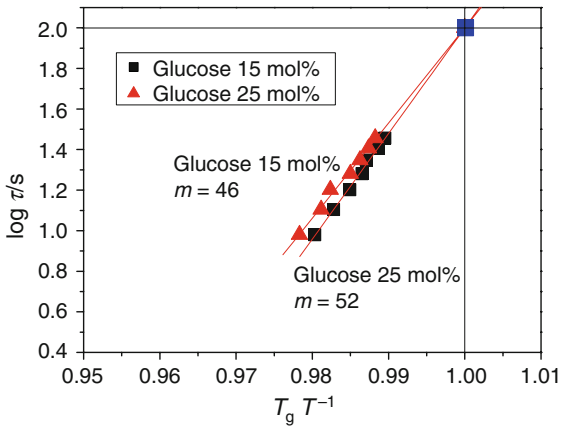


**Fig. 5** Angell plot of glucose aqueous solutions (15 and 25 mol%)

because the relaxation mode in the vicinity of $T_g$ ($0.96 < T_g/T < 1$) is investigated by the TMDSC experiments. Figure 4 shows Angell plot of EG aqueous solutions (50 and 70 mol%). It is nearly corresponding to the reported value of the past dielectric measurement about EG 50-mol% (around 80 mass/%) aqueous solution and it is suggested that the fragility of EG aqueous solution increases gradually up to the index of EG 70-mol% aqueous solution [16]. Thus, it was proven to obtain powerful and new information even if it was narrow area on the millihertz range. Additionally, as shown in Fig. 5, the fragility of glucose aqueous solutions (15 and 25 mol%) has no substantial change. It seems that the hydration structures of highly concentrated glucose aqueous solutions change only slightly with the composition. While, it will be required to measure it in wider composition range in the future.

## Elastic properties

The observed Brillouin spectra of EG 40-mol% aqueous solutions and glucose 15-mol% aqueous solutions showed one broad longitudinal acoustic (LA) mode as shown in Figs. 6a and 7a. Brillouin shift $\nu$ ($=qV_L/2\pi$) and FWHM, $\Gamma$

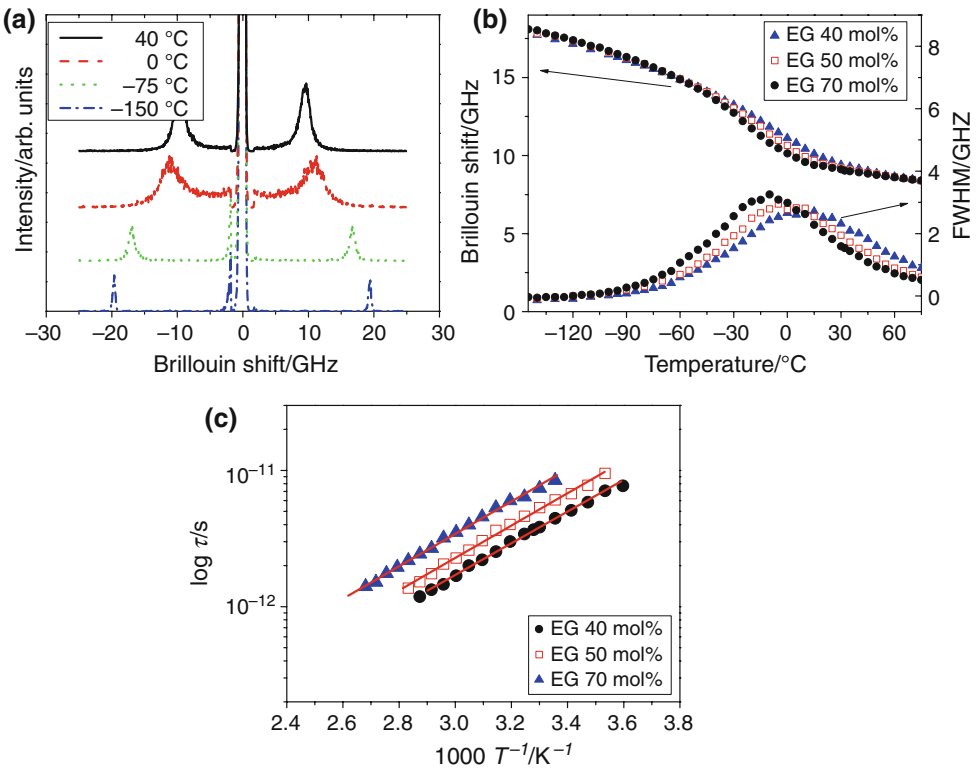


**Fig. 6** **a** Observed Brillouin-scattering spectra of EG 40 mol% aqueous solution at selected temperatures. **b** Temperature dependence of Brillouin shift and FWHM of EG aqueous solutions (40, 50, and 70 mol%). **c** Arrhenius plot of EG aqueous solutions (40, 50, and 70 mol%)

were determined from the spectra. The longitudinal sound velocity, $V_L$, was calculated from the Brillouin shift and the scattering wave vector $q$ ($=4\pi n\sin(\theta/2)/\lambda$), where $n$, $\lambda$, and $\theta$ are the values of refractive index of the sample, the wavelength of the laser, and the scattering angle, respectively. The LA mode absorption coefficient of $\alpha$ is related to a full width half maximum (FWHM) of a Brillouin component by the equation, $\alpha = \pi\Gamma/V_L$. Figures 6b and 7b showed the plot of the temperature dependences of Brillouin shift and FWHM of EG aqueous solutions (40, 50, and 70 mol%) and glucose aqueous solutions (15, 20 and 25 mol%) contained glassy glucose that is made using melt-quenching method. The temperature dependence of each solution can be discussed by the relaxation process from Debye relaxation that originated in elastic properties with the peak in the FWHM. Respectively, each temperature dependence shows the typical relaxation behavior, and the fit results of relaxation time in the Arrhenius law are shown in Figs. 6c and 7c. The relaxation time $\tau$ can be obtained by the following equation [17–20]:

$$\tau = \frac{\omega_m}{\omega^2}\left\{\left(\frac{\Delta\Gamma_m}{\Delta\Gamma}\right) + \sqrt{\left(\frac{\Delta\Gamma_m}{\Delta\Gamma}\right)^2 - \left(\frac{\omega}{\omega_m}\right)^2}\right\} (T < T_m), \quad (5)$$

where $\omega_m$, $\tau$, and $\Delta\Gamma_m$ are the maximum angular frequency, relaxation time, and maximum value of FWHM, respectively. The attempt frequency $f_0$, attempt relaxation time $\tau_0$, and activation energy $\Delta E$ were determined by the Arrhenius equation, $\tau = \tau_0\exp(\Delta E/RT)$. This value was compared with the parameter of the pure water [21].

Table 1 shows the relaxation parameters of pure water and each EG aqueous solution (40, 50, and 70 mol%). The relaxation parameters of each EG aqueous solution are nearly equal. According to the comparison of the relaxation times between pure water and EG aqueous solutions, the obtained molecular motion of EG aqueous solution can move faster than hydrogen bonded pure water. Therefore, it means that the obtained motion of EG solution is not the slow $\alpha$-relaxation [22, 23], but the local motion such as the slow $\beta$-relaxation, which is weakly coupled to the cooperative rearrangement regions related to the $\alpha$-relaxation. Table 2 which shows the relaxation parameters of pure water and each glucose aqueous solution (15, 20, and 25 mol%) indicates that the relaxation times of glucose aqueous solutions were slower than that of pure water. It seems that the marked difference between EG and glucose aqueous solutions may be originated from the coexistence of three kinds of isomers of glucose. Glucose molecules in aqueous solution exist in equilibrium between chain and cyclic structures, while EG molecules in aqueous solution take only chain structure. Therefore, there is the possibility that the equilibrium of glucose in aqueous solution enhance to move cooperatively with water molecules.

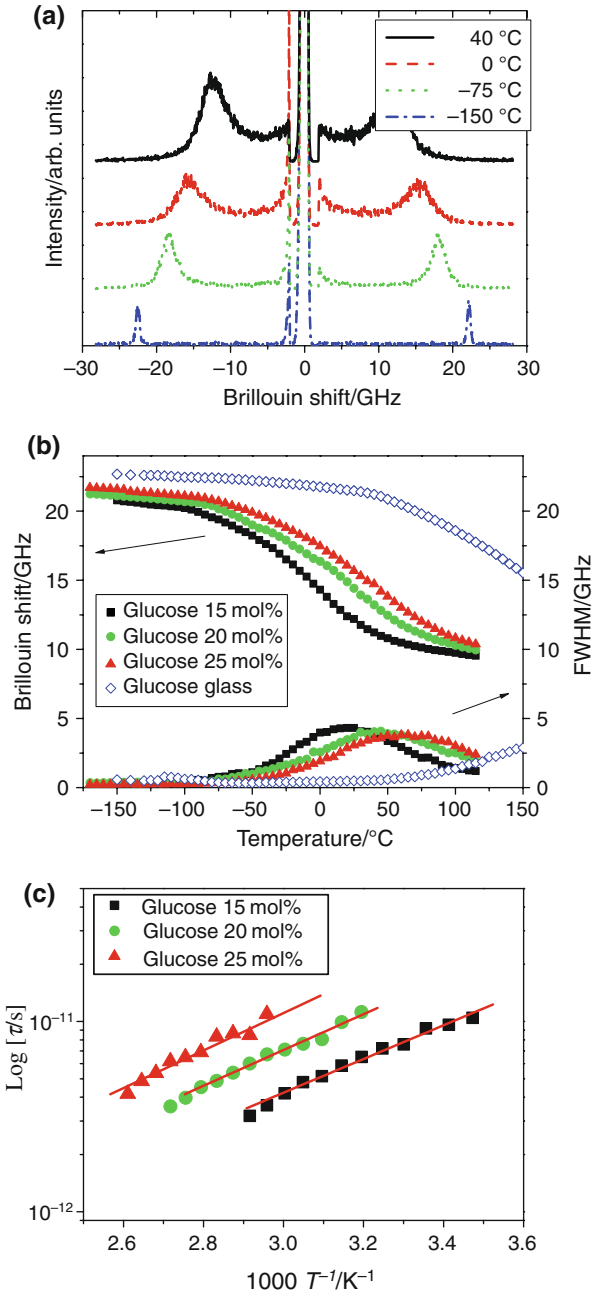


**Fig. 7** **a** Observed Brillouin-scattering spectra of glucose 15-mol% aqueous solution at selected temperatures. **b** Temperature dependence of Brillouin shift and FWHM of glucose aqueous solutions (15, 20, and 25 mol%) and glassy glucose. **c** Arrhenius plot of glucose aqueous solutions (15, 20, and 25 mol%)

**Table 1** Values of parameters of EG aqueous solutions (40, 50, and 70 mol%) and pure water

| | $f_0$/Hz | $\tau_0$/s | $\Delta E$/kJ/mol |
|---|---|---|---|
| Pure water [21] | $5.3 \times 10^{13}$ | $(3 \pm 2) \times 10^{-15}$ | $16 \pm 3$ |
| EG 40 mol% | $2.9 \times 10^{14}$ | $(5.5 \pm 0.9) \times 10^{-16}$ | $22 \pm 1$ |
| EG 50 mol% | $2.6 \times 10^{14}$ | $(6.2 \pm 1.4) \times 10^{-16}$ | $23 \pm 1$ |
| EG 70 mol% | $1.7 \times 10^{14}$ | $(9.2 \pm 1.4) \times 10^{-16}$ | $23 \pm 1$ |

**Table 2** Values of parameters of glucose aqueous solutions (15, 20, and 25 mol%) and pure water

| | $f_0$/Hz | $\tau_0$/s | $\Delta E$/kJ/mol |
|---|---|---|---|
| Pure water [21] | $5.3 \times 10^{13}$ | $(3 \pm 2) \times 10^{-15}$ | $16 \pm 3$ |
| Glucose 15 mol% | $1.7 \times 10^{13}$ | $(9.2 \pm 0.3) \times 10^{-15}$ | $17 \pm 1$ |
| Glucose 20 mol% | $1.5 \times 10^{13}$ | $(1.0 \pm 0.4) \times 10^{-14}$ | $18 \pm 1$ |
| Glucose 25 mol% | $1.3 \times 10^{13}$ | $(1.2 \pm 0.7) \times 10^{-14}$ | $19 \pm 1$ |

## Conclusions

We studied the dynamical properties of giga- and millihertz ranges of EG aqueous solutions and highly concentrated glucose aqueous solutions. The fragility of each aqueous solution has been investigated by TMDSC. The α-relaxation time and peak temperature of imaginary part of complex specific heat were analyzed by Angell plot. Then, the fragility index $m$ was determined from the slope of the Angell plot. In the gigahertz range, we determined the relaxation times of aqueous solutions under the assumption of Debye relaxation that related to elastic properties. According to the relaxation times of EG aqueous solution, it seems that the molecular motion of EG aqueous solution can move faster than pure water. In contrast, the relaxation times of glucose aqueous solution were slower than that of pure water, probably due to the coexistence of three kinds of isomers of glucose.

**Acknowledgements** This research was partially supported by the Ministry of Education, Science, Sports and Culture, Grants-in-Aid for Exploratory Research, 19656005, 2008 and the Research Foundation of the Japan Society for the Promotion of Science for Young Scientists, 18-3811, 2008.

## References

1. Baudot A, Odagescu V. Thermal properties of ethylene glycol aqueous solutions. Cryobiology. 2004;48:283–94.
2. Bulone D, Donato ID, Palma-Vittorelli MB, Palma MU. Density, structural lifetime, and entropy of H-bond cages promoted by monohydric alcohols in normal and supercooled water. J Chem Phys. 1991;94:6816–26.
3. Gao C, Zhou G, Xu Y, Hua TC. Glass transition and enthalpy relaxation of ethylene glycol and its aqueous solution. Thermochem Acta. 2005;435:38–43.
4. Hancock BC, Shamblin SL, Zografi G. Molecular mobility of amorphous pharmaceutical solids below their glass transition temperatures. Pharm Res. 1986;12:799–806.
5. Hancock BC, Zografi G. Characteristics and significance of the amorphous state in pharmaceutical systems. J Pharm Sci. 1997;86:1–12.
6. Deeney FA, O'leary JP, Cronin B, O'leary DM. The effects of quantum zero point energy fluctuations on the variation with concentration of the maximum density temperatures in water–alcohol solutions. Chem Phys Lett. 2008;465:216–9.

7. Seshimo Y, Ike Y, Kojima S. Brillouin scattering study of cluster structure in lower alcohol water mixtures. Jpn J Appl Phys. 2008;47:3836–38.
8. Ike Y, Seshimo Y, Kojima S. Complex heat capacity of non-Debye process in glassy glucose and fructose. Fluid Phase Eq. 2007;256:123–6.
9. Angell CA, Ngai KL, McKenna GB, McMillan PF, Martin SW. Relaxation in glassforming liquids and amorphous solids. J Appl Phys. 2000;88:3113–57.
10. Angell CA. Relaxation in liquids, polymers and plastic crystals—strong/fragile patterns and problems. J Non-Cryst Solids. 1991;131–133:13–31.
11. Ike Y, Matsuda Y, Kojima S, Kodama M. Brillouin scattering of liquid glass transition in lithium borate glass. Jpn J Appl Phys. 2006;45:4474–8.
12. Jiang F, Kojima S. Micro-heterogeneity and relaxation in 0.65PMN-0.35PT relaxor single crystals. Appl Phys Lett. 2000; 77:1271–3.
13. Seo J-A, Kim SJ, Oh J, Kim HK, Hwang Y-H. Brillouin scattering and DSC studies of glass transition temperatures of glucose-water mixtures. J Korean Phys Soc. 2004;44:523–6.
14. Matsuda Y, Fukawa Y, Ike Y, Kodama M, Kojima S. Dynamic specific heat, glass transition, and non-Debye nature of thermal relaxation in lithium borate glasses. J Phys Soc Jpn. 2008;77: 084602.
15. Hahsimoto E, Aoki Y, Seshimo Y, Sasanuma K, Ike Y, Kojima S. Dehydration process of protein crystals by micro-Brillouin scattering. Jpn J Appl Phys. 2008;47:3839–42.
16. Sudo S, Shinyashiki N, Yagihara S. The dielectric relaxation of supercooled ethyleneglycol-water mixtures. J Mol Liq. 2001; 90:113–20.
17. Sivasubramanian V, Tsukada S, Kojima S. Brillouin scattering studies of dynamics of polar nanoregions in $Pb[(In_{1/2}Nb_{1/2})_{0.65}Ti_{0.35}]O_3$ single crystals. Jpn J Appl Phys. 2008;47:7740–4.
18. Tsukada S, Ike Y, Kano J, Kojima S. Brillouin scattering study of glass-forming propylene glycol. Mater Sci Eng A. 2006;442: 379–82.
19. Tsukada S, Kojima S. Broadband light scattering of two relaxation processes in relaxor ferroelectric $0.93Pb(Zn_{1/3}Nb_{2/3})O_3$-$0.07PbTiO_3$ single crystals. Phys Rev B. 2008;78:144106.
20. Tsukada S, Ike Y, Kano J, Kojima S. Dynamical properties of polar nanoregions of relaxor ferroelectric $Pb(Ni_{1/3}Nb_{2/3})O_3$-$0.29PbTiO_3$. J Phys Soc Jpn. 2008;77:033707.
21. Monaco G, Cunsolo A, Ruocco G, Sette F. Viscoelastic behavior of water in the terahertz-frequency range: an inelastic x-ray scattering study. Phys Rev E. 1991;60:5505–21.
22. Birge NO, Nagel SR. Specific-heat spectroscopy of the glass transition. Phys Rev Lett. 1985;54:674–77.
23. Birge NO. Specific-heat spectroscopy of glycerol and propylene glycol near the glass transition. Phys Rev B. 1986;34:1631–42.